SLAC-PUB-5824
May 1992
(A)

Transient Response of the Beam after Injection into a Storage Ring*

H. Moshammer
Stanford Linear Accelerator Center
Stanford University, Stanford, CA 94309

Abstract

The time evolution of the distribution function of a mismatched or an off-axis injected Gaussian bunch is derived from the Vlasov equation. Radiation damping as well as current dependent effects are neglected. Analytic expressions for the first and second moments of the longitudinal and transverse distributions are derived when nonlinear fields which lead to decoherence of the center of mass and to filamentation of the emittance are taken into account. Coupling between the longitudinal and the transverse planes due to chromaticity will lead to synchrotron sidebands to the betatron tune in the Fourier spectrum of the transverse center of mass motion after injection.

Introduction

In well chosen canonical coordinates and ignoring nonlinear fields the Hamiltonian of the longitudinal or the transverse single particle motion is precisely that of a harmonic oscillator and the trajectory may be represented in phase space by circles centered on the origin (closed orbit).

On the other hand, a bunch injected into a circular accelerator is not necessarily centered on the closed orbit or the injected distribution in phase space may not have circular contours. In both cases the distribution function, which describes the properties of the beam, will depend explicitly on time. Due to nonlinear fields particles in the bunch will have different frequencies of oscillation. As a consequence, the beam size will increase gradually. This process, called filamentation [2], occurs after injecting the beam in a periodic structure e.g. linacs or storage rings.

If the beam is injected off-axis, i.e. not on the closed orbit, the nonlinear fields induce different oscillation frequencies of particles with different amplitude leading to a damping in the center of mass of the beam. The center of mass is said to decohere. This effect was observed and analysed in proton storage rings when the beam had been kicked into the nonlinear regime. Higher order multipole fields and their effect on the beam were studied by these methods at the SPS and at the TEVATRON [3], [4], [5].

As a preliminary step to the understanding of the difficulties associated with the injection process, we shall discuss in this paper the evolution of the distribution function after injection. We are neglecting synchrotron radiation and collective effects such as the beam-wall interaction through wake-fields. The first two sections are devoted to the longitudinal phase space, but in Section 3 we shall obtain comparable results for the horizontal phase space.

In Section 1 we derive the distribution function after injection associated with a harmonic oscillator type Hamiltonian and constant oscillation frequency ω_0. Then we switch to action-angle variables to take into account nonlinear forces. Averaging over phase terms (see [6]) reduces the Hamiltonian to a function of the action only. The action variable itself remains an integral of motion and the effect of the nonlinear terms are described by the amplitude dependence of the oscillation frequency $\omega(I)$ [8], [7], [3], [9]. For a Hamiltonian of the type $H(I)$ the Vlasov equation does not contain a derivative w.r.t. the action variable. This symmetry

*Work supported by the Department of Energy, contract DE-AC03-76SF00515.

invokes solutions to the Vlasov equation which were derived previously for the harmonic oscillator type of Hamiltonian with ω_0 now replaced by $\omega(I)$:

$$\omega_0 = \partial H_0(I)/\partial I \qquad \rightarrow \qquad \omega(I) = \partial H(I)/\partial I$$

$$\downarrow$$

$$\Psi_0(\phi, I, \omega_0 t) \qquad \rightarrow \qquad \Psi(I, \phi, \omega(I)t)$$

In this report we focus on a Gaussian distribution at injection. Other types of distributions may be treated in a similar way.

Analytic expressions for the first and second moments of the longitudinal distribution function will be derived in Section 2. These expressions are then compared with multi-particle simulations for typical parameters of the SLC Damping Rings. The horizontal phase space will be treated in analogy to the longitudinal phase space in Section 3.

An additional source for the spread in the horizontal rotation frequency is the chromaticity which couples the longitudinal to the horizontal motion. In Section 4 we treat the decoherence of the horizontal center of mass motion $< x >$ due to nonlinear fields and chromaticity. Coupling between the longitudinal and the horizontal phase space leads to synchrotron sidebands to the betatron frequency in the Fourier spectrum of $< x >$ after injection.

Most of the integrals involved in the evaluation of the different moments of the distribution function can be looked up in integral tables. The only integral where the solution cannot be found easily will be treated in the Appendix.

If we wanted to include radiation damping or quantum excitation we would replace the Vlasov equation by the Fokker-Planck equation, which involves derivatives w.r.t. the action variable. The above mentioned symmetry would then be lost and the recipe to replace $\omega_0 \rightarrow \omega(I)$ cannot be used to obtain solutions to the Fokker-Planck Equation for the perturbed Hamiltonian $H(I)$.

1. Time Evolution of the Distribution Function in Longitudinal Phase Space

In this section we discuss the time evolution of the distribution function in longitudinal phase space after mismatched or off-axis injection. Later, in section 3, these results will be translated into the horizontal plane.

The energy spread injected into the SLC Damping Ring is about 10 times larger than the equilibrium energy spread and the bunch length at injection is smaller than at equilibrium. This apparent mismatch at injection motivates the definition of the parameter g:

$$g = \frac{\sigma_{z0}\sigma_{\epsilon\infty}}{\sigma_{\epsilon 0}\sigma_{z\infty}} = \frac{\sigma_{z0}\nu_s}{\sigma_{\epsilon 0}\alpha R} ,$$

where we denote the injected sizes by σ_{z0} and $\sigma_{\epsilon 0}$, α is the momentum compaction factor, ν_s is the synchrotron tune and $\sigma_{z\infty}$ and $\sigma_{\epsilon\infty}$ denote the bunch length or energy spread at equilibrium. A matched injected distribution would allow $g = 1$. The single particle motion may be described by the Hamiltonian function [7]:

$$H(\epsilon, z) = \alpha \left[\frac{\epsilon^2}{2} + \frac{\nu_{s0}^2}{\alpha^2 R^2} \left(\frac{z^2}{2} - \tan(\phi_s) \frac{h}{R} \frac{z^3}{3!} - \frac{h^2}{R^2} \frac{z^4}{4!} \right) \right] + \cdots \tag{1}$$

where R denotes the mean radius of the ring and the nonlinear terms originate from the expansion of the sinusoidal RF waveform around the synchronous phase ϕ_s. For $g = 1$ the distribution in normalized coordinates $(\epsilon/\sigma_{\epsilon\infty}, z/\sigma_{z\infty})$ remains circular. For $g \neq 1$ we expect to see a rotating ellipse, at least in the absence of nonlinear driving terms. The distribution function:

$$\Psi_0(t) = \frac{1}{2\pi A} \exp\left(-\frac{c(t)\epsilon^2 - 2a(t)z\epsilon + b(t)z^2}{2A^2}\right) , \tag{2}$$

contains the geometric expression of a rotating ellipse in the exponent. The quantities $a(t), b(t), c(t)$ have to satisfy the Vlasov equation.

$$\frac{\partial \Psi_0}{\partial s} + [H_0, \Psi_0] = 0 \quad \text{with:} \quad H_0 = \frac{\alpha}{2}\left(\epsilon^2 + \frac{\nu_{s0}^2}{\alpha^2 R^2} z^2\right) .$$

We first ignore the nonlinear terms in the Hamiltonian. As a solution to the Vlasov equation we obtain:

$$\begin{aligned} A &= \sigma_{z0}\sigma_{\epsilon 0} \\ c(t) &= \frac{1}{2g^2}\sigma_{z0}^2(1 + g^2 + (g^2 - 1)\cos(2\omega_{s0}t)) \\ b(t) &= \frac{1}{2}\sigma_{\epsilon 0}^2(1 + g^2 - (g^2 - 1)\cos(2\omega_{s0}t)) \\ a(t) &= \frac{1}{2g}\sigma_{\epsilon 0}\sigma_{z0}(g^2 - 1)\sin(2\omega_{s0}t)) . \end{aligned} \tag{3}$$

The off-axis injection is taken into account by changing the origin of the ellipsoid in the distribution function.

$$\Psi_0(t) = \frac{1}{2\pi A}\exp\left(-\frac{c(t)(\epsilon - \hat{\epsilon})^2 - 2a(t)(z - \hat{z})(\epsilon - \hat{\epsilon}) + b(t)(z - \hat{z})^2}{2A^2}\right) , \tag{4}$$

where $(\hat{\epsilon}(t), \hat{z}(t))$ describes the time evolution of the injected center of mass. Later when we add the nonlinear terms we shall realize that the trajectory which originates at the center of mass at injection will not describe the center of mass motion after injection. The distribution function given in Eq. 4 satisfies the Vlasov Equation provided the time evolution of $(\hat{\epsilon}(t), \hat{z}(t))$ is defined by Hamilton's Equations:

$$\hat{\epsilon}(t) = \epsilon_0 \cos(\omega_s t) + \frac{\nu_{s0}}{R\alpha} z_0 \sin(\omega_s t)$$

$$\hat{z}(t) = -\frac{\nu_{s0}}{R\alpha}\epsilon_0 \sin(\omega_s t) + z_0 \sin(\omega_s t) ,$$

where ϵ_0, z_0 denote the coordinates of the center of mass at the moment of injection (t=0). Next we take into account the nonlinear terms in the Hamiltonian. A convenient way to deal with the nonlinear perturbation in the Hamiltonian of Eq. 1 is to switch to action-angle variables (ϕ, I). Hamilton-Jacobi perturbation technique leads to a new averaged Hamiltonian which depends only on the action variable [10], [7]:

$$H_a(I) = \frac{\nu_{s0}}{R}(I - \frac{\mu}{2}I^2) \quad \text{with:} \quad \mu = \frac{h^2\alpha}{8R\nu_{s0}}\left(1 + \frac{5}{3}\tan(\phi_s)^2\right) . \tag{5}$$

For example in the SLC Damping Ring we have $\mu \approx 450$ in the zero current limit. The main contribution in μ originates from the term z^4 of the Hamiltonian in Eq. 1 and may be extracted by averaging over phase terms in Eq. 1. The second term containing the tangent of the synchronous phase originates from a second order contribution of z^3.

It should be stressed at this point that the solution obtained with the average Hamiltonian $H_a(I)$ will deviate from the original problem described by the Hamiltonian in Eq. 1. The frequency of oscillation and thus the synchrotron tune depends now on the amplitude I:

$$\nu_s(I) = R\frac{dH_a(I)}{dI} = \nu_{s0}(1 - \mu I) . \tag{6}$$

The distribution function in action-angle variables is obtained from Eq. 4 by the canonical transformation:

$$z = \sqrt{\frac{2I\alpha R}{\nu_{s0}}}\cos(\phi) \quad \text{and} \quad \epsilon = \sqrt{\frac{2I\nu_{s0}}{\alpha R}}\sin(\phi) . \tag{7}$$

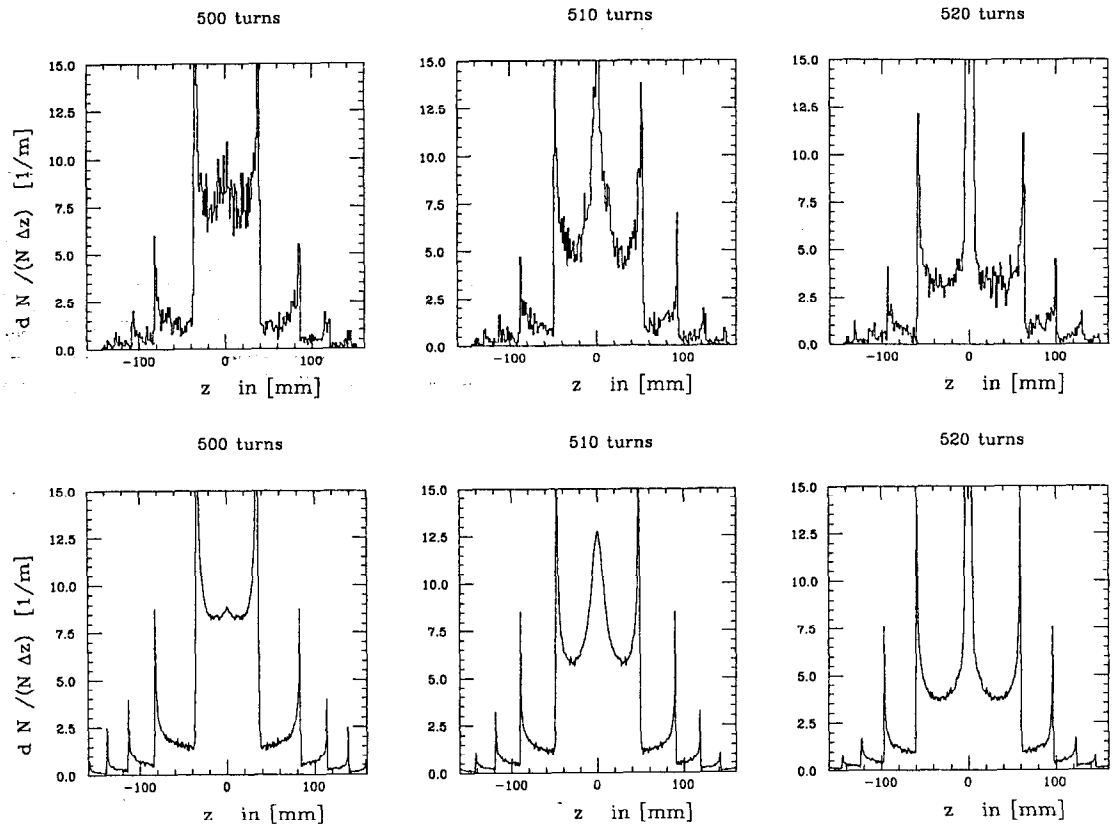

Figure 1 Longitudinal density distribution from simulation (top) and from Eq. 10

To include the nonlinear fields we convert Eq. 4 to action-angle variables and replace the oscillation frequency by the expression 6.

$$\Psi(t) = \frac{1}{2\pi A}\exp(-\frac{[\sqrt{I}\cos(\phi-\omega_s(I)t)-\sqrt{I_0}\cos(\phi_0)]^2+g^2[\sqrt{I}\sin(\phi-\omega_s(I)t)-\sqrt{I_0}\sin(\phi_0)]^2}{g\sigma_{z0}\sigma_{\epsilon 0}} \tag{8}$$

I_0, ϕ_0 denote the position of the center of mass at the moment of injection:

$$\tan(\phi_0) = \frac{\alpha R}{\nu_{s0}}\frac{\epsilon_0}{z_0} \quad , \qquad I_0 = \frac{1}{2}(\frac{\nu_{s0}}{\alpha R}z_0^2 + \frac{\alpha R}{\nu_{s0}}\epsilon_0^2) \; .$$

The distribution function 8 satisfies the Vlasov Equation with the new Hamiltonian:

$$\frac{\partial \Psi}{\partial s} + \frac{\nu_s(I)}{R}\frac{\partial \Psi}{\partial \phi} = 0 \; . \tag{9}$$

At this point it is interesting to compare the distribution function in Eq. 8 with multi-particle simulation for the longitudinal density distribution, i.e. the projection of the distribution function on the longitudinal axis. We choose the case of a centered, $I_0 = 0$, but strongly mismatched beam, $g = 1/25$, as it is the case at the SLC Damping Ring. To evaluate the longitudinal density distribution we have to evaluate the integral:

$$\rho(z,t) = \int_{-\infty}^{\infty} \Psi(t) d\epsilon \; . \tag{10}$$

Although $\Psi(t)$ is a relatively simple analytic expression, this integral could not be solved analytically. Nevertheless the numerical integration is straightforward and was done at turn number 500, 510 and 520 after injection.

We compare these results to the longitudinal density distribution obtained by a simulation code. The one turn map consists of:

$$\Delta\epsilon = -\frac{eV_{RF}}{E_0}\left[\sin(\phi_s - \frac{h}{R}z) - \sin(\phi_s)\right] \quad \text{and:} \quad \Delta z = -\alpha\epsilon$$

8000 particles were tracked for the same number of turns, 500 to 520, and the integration in Eq. 10 was replaced by counting the number of particles in a small interval Δz along the longitudinal axis z. The longitudinal density distributions obtained by both methods are shown in Fig. 1 (top and bottom). Due to the amplitude dependent tune the distribution starts to spiral in phase space. The spiral shaped distribution causes the spikes shown in Fig. 1 when projected on the $z-$axis. The density distribution obtained form the multi-particle simulation shows fairly good agreement with the distribution evaluated from the integration of Eq. 8.

2 First and second Moments of the Longitudinal Distribution Function

Next we derive analytic expressions for the first and second moment of the longitudinal distribution. We distinguish between two special cases: a) mismatched beam is injected on-axis ($g \neq 1, I_0 = 0$), and b) matched beam is injected off-axis ($g = 1, I_0 \neq 0$).

2.a Mismatched Beam injected On-Axis

With $I_0 = 0$ the first moment vanishes. The second moment is associated with the bunch length and can be evaluated analytically. The distribution function in Eq. 8 simplifies to:

$$\Psi(t)_{(I_0=0)} = \frac{1}{2\pi A}\exp\left(-\frac{I\cos(\phi-\omega_s(I)t)^2 + g^2 I\sin(\phi-\omega_s(I)t)^2}{g\sigma_{z0}\sigma_{\epsilon 0}}\right) . \tag{11}$$

We first perform the integration w.r.t. the angle variable ϕ which yields the solution in terms of Bessel functions [11]:

$$< z^2 >= \frac{\alpha R}{\sigma_{z0}\sigma_{\epsilon 0}\nu_{s0}}\int_0^{I_{max}} dI\, I\exp(-I\frac{1+g^2}{2g\sigma_{z0}\sigma_{\epsilon 0}})[J_0(iI\frac{1-g^2}{2g\sigma_{z0}\sigma_{\epsilon 0}}) + i\cos(2\omega_s(I)t)J_1(iI\frac{1-g^2}{2g\sigma_{z0}\sigma_{\epsilon 0}})] ,$$

where i denotes the imaginary unit and I_{max} determines the cut-off amplitude value of the initial distribution. Usually this value is determined by the energy acceptance of the ring. If we allow some of the incoming particles to overcome the potential well provided by the RF and use $I_{max} = \infty$ the upper integral becomes:

$$< z^2 >_{I_0=0} = \frac{\sigma_{z0}^2}{2g^2}\left[1 + g^2 + (g^2-1)\Big(\Re\{Z(t)^{3/2}\}\cos(2\omega_{s0}t) + \Im\{Z(t)^{3/2}\sin(2\omega_{s0}t)\}\Big)\right] , \tag{12}$$

$$\text{with :} \quad Z(t) = \frac{1}{1 - 4\theta^2 + i(1+g^2)2\theta/g} \quad \text{and :} \quad \theta = \mu\sigma_{z0}\sigma_{\epsilon 0}\omega_s t \ .$$

The complex quantity $Z(t)$ acts like a damping term. With increasing t the real and the imaginary parts $\Re\{Z(t)\}, \Im\{Z(t)\}$ decrease. The asymptotic value $t = \infty$ gives the blow up of the bunch length due to filamentation:

$$< z^2 >_{t\to\infty} = \frac{\sigma_{z0}^2}{2g^2}(1+g^2) .$$

Even after a sufficient number of revolutions the distribution is not Gaussian in the coordinates z, ϵ. The different layers of the spiraling distribution (filaments) will approach one another. But the area of the injected ellipse which corresponds to the normalization variable A, will remain constant throughout the filamentation process as it is required by Liouville's theorem.

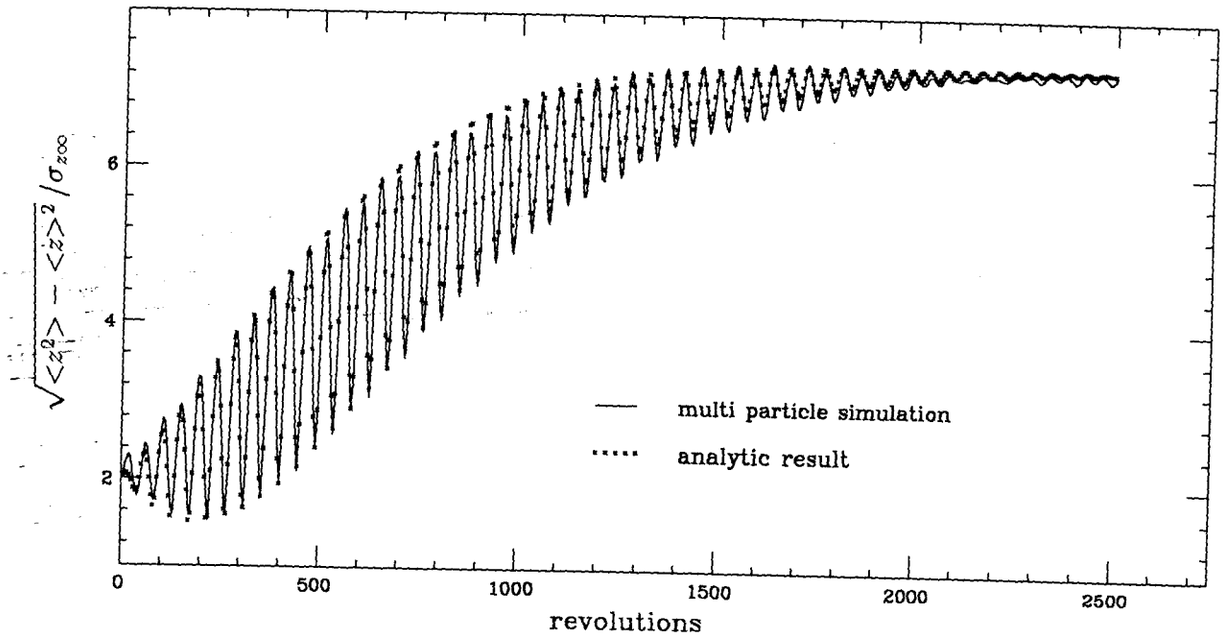

Figure 2 Evolution of the bunch length after injection

2.b Matched Beam injected Off-Axis

For a matched beam injected off-axis ($g = 1$) the distribution function in Eq. 8 becomes:

$$\Psi(t) = \frac{1}{2\pi A}\exp\left(-\frac{I + I_0 - 2\sqrt{II_0}\cos(\phi - \omega_s(I)t - \phi_0)}{\sigma_{z0}\sigma_{\epsilon 0}}\right). \tag{13}$$

To evaluate the first moment of this distribution we integrate first over the angle variable and obtain an expression containing Laguerre polynomials [11]. The second integration is done over the action variable and leads to:

$$< z >= \frac{\sqrt{\frac{2\alpha R I_0}{\nu_{s0}}}\, e^{-\frac{\theta^2 I_0}{(1+\theta^2)\sigma_{z0}\sigma_{\epsilon 0}}}}{(1+\theta^2)^2}\left[(1-\theta^2)\cos(\omega_{s0}t + \phi_0 - \frac{\theta I_0}{(1+\theta^2)\sigma_{z0}\sigma_{\epsilon 0}}) + 2\theta\sin(\omega_{s0}t + \phi_0 - \frac{\theta I_0}{(1+\theta^2)\sigma_{z0}\sigma_{\epsilon 0}})\right] \tag{14}$$

As we expected we observe a damping of the center of mass towards the origin of phase space in the limit of $t \to \infty$. It is worth to mention that the damping occurs not purely exponentially as in the case of radiation damping. In a similar way we calculate the time evolution of the second moment:

$$< z^2 >= \sigma_{z0}^2 + \frac{\sigma_{z0}}{\sigma_{\epsilon 0}} I_0\left[1 + \frac{e^{-\frac{4 I_0 \theta^2}{\sigma_{z0}\sigma_{\epsilon 0}(1+4\theta^2)}}}{(1+4\theta^2)^3}\{(1-12\theta^2)\cos(2\Phi_4) - (6\theta - 8\theta^3)\sin(2\Phi_4)\}\right] \tag{15}$$

and the phases are given by:

$$\Phi_1 = \omega_{s0}t + \phi_0 - \frac{\theta I_0}{\sigma_{z0}\sigma_{\epsilon 0}(1+\theta^2)} \quad \text{with} \quad \Phi_4 = \omega_{s0}t + \phi_0 - \frac{\theta I_0}{\sigma_{z0}\sigma_{\epsilon 0}(1+4\theta^2)}$$

The equilibrium value reached after a sufficient large number of turns is given by:

$$(< z^2 > - < z >^2)_{t=\infty} = \sigma_{z0}^2 + \frac{\sigma_{z0}}{\sigma_{\epsilon 0}} I_0 \tag{16}$$

gure 2 shows as an example the second moment extracted from a multi-particle simulation (solid line) and e analytic result of Eq. 15 (indicated by stars). There are three reasons why we see small deviations between ulation and analytic result:

- The simulated particle distribution at injection is not exactly Gaussian. In the absence of nonlinear fields the bunch length varies by about 2 %. I was using 5000 test particles.
- The simulation is done in two discrete steps: Map 1 over the ARC, Map 2 at the RF cavity whereas the Hamiltonian is based on differential equations which assumes the RF cavities to be spread over the ARC.
- The distribution function is based on an averaged Hamiltonian which has lost the phase information with respect to the original Hamiltonian $H(\epsilon, z)$ in Eq. 1. This difference should smooth out after a couple of synchrotron oscillations. Hence, we expect a discrepancy within the first synchronous oscillation which is clearly visible in Fig. 2 between turn number 1 and 25 (one synchrotron oscillation corresponds to about 100 turns).

3 First and second Moments of the Horizontal Distribution Function

In this section we derive analytic expressions for the horizontal time evolution of the center of mass and the horizontal beam size after injection. The single particle motion may be described by the Hamiltonian [8]:

$$H = \frac{1}{2}p^2 + \frac{1}{2}K_1(s)x^2 + \frac{1}{3!}K_2(s)x^3 + \frac{1}{4!}K_3(s)x^4 \ , \tag{17}$$

where $K_1(s), K_2(s)$ and $K_3(s)$ describe the distribution of the magnetic quadrupoles, sextupoles and octupoles around the ring and x denotes the betatron displacement from the closed orbit. We introduce a new set of canonical variables:

$$x_n = \frac{x}{\sqrt{\beta(s)}} \quad , \quad p_n = \frac{\alpha(s)}{\sqrt{\beta(s)}}x + \sqrt{\beta(s)}p$$

If we are interested in the distribution function at a single location of the ring and not in the evolution of the distribution function around the ring the Hamiltonian simplifies by another canonical transformation to:

$$H = \frac{\nu_{x0}}{2R}(p_n^2 + x_n^2) + \frac{1}{3!}K_2(s)\beta(s)^{3/2}x_n^3 + \frac{1}{4!}K_3(s)\beta^2(s)x_n^4 \ .$$

We switch to action-angle variables:

$$p_n = \sqrt{2I}\cos(\phi) \quad , \quad x_n = \sqrt{2I}\sin(\phi) \ . \tag{18}$$

We notice that the Hamilton-Jacobi perturbation technique has already been used to obtain the new Hamiltonian solely in action variables [3], [8]:

$$H_a(I) = \frac{\nu_{x0}}{R}(I - \frac{1}{2}(\mu_2 + \mu_3)I^2) \ \text{ and } \ \nu_x(I) = R\frac{dH_a(I)}{dI} = \nu_{x0}\,(1 - (\mu_2 + \mu_3)I) \ .$$

with:

$$\begin{aligned} \mu_2 &= \frac{1}{64\nu_x\pi}\oint ds\beta(s)^{3/2}K_2(s)\int_s^{s+C}\beta(s')^{3/2}K_2(s')ds' \\ &\times \left\{\frac{3\cos(\psi(s') - \psi(s) - \pi\nu_x)}{\sin(\pi\nu_x)} + \frac{\cos(3\psi(s') - 3\psi(s) - 3\pi\nu_x)}{\sin(3\pi\nu_x)}\right\} , \end{aligned} \tag{19}$$

$$\mu_3 = -\frac{1}{16\nu_x\pi}\oint ds\beta(s)^2K_3(s) \ , \tag{20}$$

where $\psi(s)$ denotes the betatron phase advance. Similar to the longitudinal case we have two contributions to the nonlinear tune shift. The octupoles give a first order term and the sextupoles contribute in second order similar to the tangent of the synchronous phase in Eq. 5. Tracking of two particles with different amplitudes

provides an alternative method to obtain the amplitude dependence of the tune. I used MAD [12] to track two particles for 100 turns. It is necessary to average over the fluctuating part to obtain the tune shift plotted in Fig. 3 as a function of the tune. A model of the SLC damping ring without octupoles was used. The stars denote the tune shift extracted from the tracking and the solid line correspond to the analytic expression in Eq. 19. The small deviation between analytic result and tracking is probably due to second-order contributions from the main bending magnets. The 1/3 resonance is compensated fairly well by a carefully chosen sextupole configuration in the original design of the ring [13].

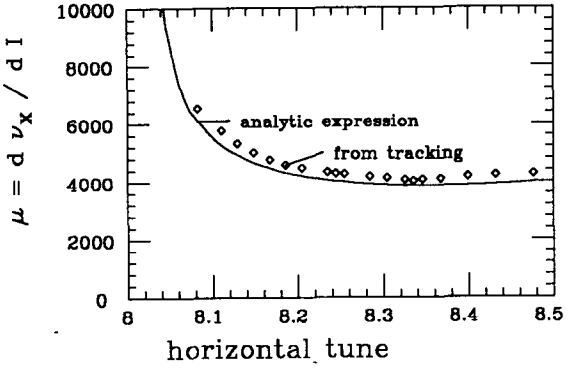

Figure 3 Tune dependance on the amplitude of the oscillation

3.a Mismatched Beam injected On-Axis

In the physical coordinates (x, p) we parameterize the mismatched injected distribution with $\alpha_0, \beta_0, \epsilon_{x0}$. Then, at the moment of injection we obtain the distribution function in normalized variables (x_n, p_n) as:

$$\Psi_0(t=0) = \frac{1}{2\pi\epsilon_{x0}} \exp(-\frac{c_0 x_n^2 + 2a_0 x_n p_n + b_0 p_n^2}{2\epsilon_{x0}}) \tag{21}$$

with

$$a_0 = \alpha_0 - \frac{\beta_0}{\beta}\alpha \quad , \quad b_0 = \frac{\beta_0}{\beta} \quad \text{and} \quad c_0 = \frac{(a_0^2+1)}{b_0}$$

where α, β denote the twiss parameters of the ring at the location of interest. We try to use a similar expression to Eq. 2

$$\Psi_0(t) = \frac{1}{2\pi\epsilon_{x0}} \exp(-\frac{c(t) x_n^2 + 2a(t) x_n p_n + b(t) p_n^2}{2\epsilon_{x0}}) \tag{22}$$

and determine $c(t), a(t), b(t)$ from the Vlasov equation containing the unperturbed Hamiltonian:

$$\begin{aligned} c(t) &= -B\cos(2\omega_x t + \bar{\phi}) + C \\ b(t) &= B\cos(2\omega_x t + \bar{\phi}) + C \\ a(t) &= -B\sin(2\omega_x t + \bar{\phi}) \end{aligned} \tag{23}$$

where the constants $B, C, \bar{\phi}$ have to be determined from the twiss parameters:

$$C = \frac{1 + a_0^2 + b_0^2}{2b_0} \quad , \quad B = -\sqrt{C^2 - 1} \quad \text{and} \quad \tan(\bar{\phi}) = -\frac{2a_0 b_0}{1 + a_0^2 - b_0^2}$$

It seems that the parameterization of the transverse case is more complicated than in the longitudinal case. But unlike in the longitudinal case we allow here initial distributions which are described by tilted ellipses in phase space (x_n, p_n) which corresponds to $a(t=0) = a_0 \neq 0$. In the longitudinal distribution we implied $a(t=0) = 0$ in Eq. 4. The distribution in action-angle variables may be obtained with Eqs. 18:

$$\Psi(t) = \frac{1}{2\pi\epsilon_{x0}} \exp(-\frac{I}{\epsilon_{x0}} \{B\cos(2\phi - 2\omega_x(I)t - \bar{\phi}) + C\}) \tag{24}$$

One immediately realizes the similarity with Eq. 11. We have to substitute:

$$B = \frac{1-g^2}{2g} \quad , \quad C = \frac{1+g^2}{2g} \quad \text{and} \quad \epsilon_{x0} = \sigma_{z0}\sigma_{\epsilon 0}$$

into the results derived for the longitudinal case. Thus the second moment for on-axis injection is given by:

$$< x^2 >= \epsilon_{x0}\beta \left[C + B(\ \Re\{Z(t)^{3/2}\}\cos(2\omega_{x0}t + \bar{\phi}) + \ \Im\{Z(t)^{3/2}\}\sin(2\omega_{x0}t + \bar{\phi})\ )\right] \tag{25}$$

$$\text{with :} \quad Z(t) = \frac{1}{1 - 4\theta^2 + i4C\theta} \qquad \text{and :} \quad \theta = \mu\epsilon_{x0}\omega_x t$$

In the limit of $t \to \infty$ we obtain the increase of the beam size growth due to filamentation after mismatched injection:

$$< x^2 >_{t\to\infty} = \epsilon_{x0}\beta\frac{1 + a_0^2 + b_0^2}{2b_0} = \frac{1}{2}\epsilon_{x0}\beta\left\{\frac{\beta}{\beta_0} + \frac{\beta_0}{\beta} + \frac{\beta}{\beta_0}(\alpha_0 - \frac{\beta_0}{\beta}\alpha)^2\right\} \equiv \epsilon_{x0}\beta\beta_{mag}\ . \tag{26}$$

This asymptotic relation quantifies the apparently increased emittance due to filamentation. The quantity β_{mag} the $\beta-$mismatch parameter was introduced by Ref. [14], and is used during operation to minimize the emittance in the SLC linac [15].

3.b Matched Beam is injected Off-Axis

To derive the horizontal distribution function for off-axis injection we shift the canonical variables in Eq. 22 by the trajectory which originates in the center of mass at injection, (x_{n0}, p_{n0}), or in action angle variables (I_0, ϕ_0). Now the distribution function is given by:

$$\Psi(t) = \frac{1}{2\pi\epsilon_{x0}} e^{-\frac{1}{\epsilon_{x0}}\left\{B\left[I\cos(2\phi - 2\omega_x t - \bar{\phi}) - 2\sqrt{II_0}\cos(\phi - \phi_0 - \omega_x t - \bar{\phi}) + I_0\cos(2\phi_0 - \bar{\phi})\right] + C\left[I + I_0 - 2\sqrt{II_0}\cos(\phi - \phi_0 - \omega_x t - \bar{\phi})\right]\right\}} \tag{27}$$

An off-axis but matched beam is parameterized by $B = 0, C = 1$.

$$\Psi(t) = \frac{1}{2\pi\epsilon_{x0}} \exp(-\frac{\{I + I_0 - 2\sqrt{II_0}\cos(\phi - \omega_x(I)t - \phi_0)\}}{\epsilon_{x0}})\ , \tag{28}$$

which compares to Eq. 13. The expression we obtain for the first moment and second moment are similar to Eqs. 14, 15:

$$< x >= \frac{\sqrt{2I_0\beta}}{(1+\theta^2)^2} e^{-\frac{\theta^2 I_0}{(1+\theta^2)\epsilon_{x0}}} \left[(1-\theta^2)\sin(\Phi_1) - 2\theta\cos(\Phi_1)\right] \tag{29}$$

and:

$$< x^2 >= \epsilon_{x0}\beta + \beta I_0\Big[1 - \frac{e^{-\frac{4I_0\theta^2}{\epsilon_{x0}(1+4\theta^2)}}}{(1+4\theta^2)^3}\{(1 - 12\theta^2)\cos(2\Phi_4) + (6\theta - 8\theta^3)\sin(2\Phi_4)\}\Big] \tag{30}$$

where the phases are given by:

$$\Phi_1 = \omega_{x0}t + \phi_0 - \frac{\theta I_0}{\epsilon_{x0}(1+\theta^2)} \qquad \text{and} \qquad \Phi_4 = \omega_{x0}t + \phi_0 - \frac{\theta I_0}{\epsilon_{x0}(1+4\theta^2)}$$

If we use the initial conditions $\phi_0 = \pi/2$ Eq. 29 describes the decoherence of the bunch center after it has been kicked into a nonlinear regime. The same relation as shown in Eq. 29 has been derived in Ref. [5] using a stationary particle distribution (see also Ref. [3]).

From the second moment given by Eq. 30 we observe an increase of the beam size due to filamentation after off-axis injection: $\epsilon_{x0} \rightarrow \epsilon_{x0} + I_0$. At this point we want to illustrate the problem with a realistic example. A typical number for the injected emittance into the e^- damping ring is 10^{-7} m. Suppose we inject a beam 1 mm away from the closed orbit. With a β-function of about 4 meter at the injection point we have: $I_0 = 1/8\,10^{-6}\,m$, and the beam size will be enhanced by 50 % of it's initial value.

4. Decoherence of the Transverse Motion due to Chromaticity

Up to this point we considered betatron tune spread only due to transverse nonlinear fields. There may be an additional betatron tune spread due to the energy spread of the beam which couples via chromaticity to the betatron tune. This effect has already been treated in Ref. [5] for a matched ($g = 1$) and centered $I_0 = 0$ longitudinal distribution function neglecting nonlinear terms of the RF wave. We want to derive the center of mass motion for a mismatched $g \neq 1$ but centered $I_0 = 0$ longitudinal distribution function, where we include the nonlinear RF field as discussed in section 1.

The transverse tune depends now on the amplitude of the transverse action variable and on the relative energy deviation of the particle.

$$\nu_x = \nu_{x0}(1 - \mu I_x) + \xi\epsilon \ ,$$

where ξ denotes the chromaticity. The tune difference after some elapsed time $(t - t_0)$ may be expressed by means of Hamilton's Equations:

$$\begin{aligned}
\int \nu_x dt &= \nu_{x0}(1 - \mu I_x)(t - t_0) + \xi \int_{t_0}^{t} dt\epsilon \\
&= \nu_{x0}(1 - \mu I_x)(t - t_0) - \xi\frac{z - z_0}{c\alpha} \qquad (31) \\
&= \nu_{x0}(1 - \mu I_x)(t - t_0) - \frac{\xi}{c}\sqrt{\frac{2I_z R}{\alpha\nu_s}}\Big[\cos(\phi) - \cos(\phi - \omega_s(I_z)t)\Big] \qquad (32)
\end{aligned}$$

Where we replaced z, z_0 by the longitudinal action-angle variables ϕ_z, I_z using Eqs. 7. The center of mass motion is given by integrating over the distribution functions.

$$< x >= \int\int\int\int dI_x\, d\phi_x\, dI_z\, d\phi_z \Psi_x(t)\Psi_z(t)\, x$$

For the transverse distribution function $\Psi_x(t)$ we choose the off-centered case given in Eq. 28 and for the longitudinal phase space we use the mismatched but centered distribution function given by Eq. 11. The integration over the transverse phase space is similar to the integration leading to Eq. 29. In combination with Eq. 31 we obtain:

$$< x >= \frac{\sqrt{2I_{x0}\beta}}{(1+\theta_x^2)^2} e^{-\frac{\theta_x^2 I_0}{(1+\theta_x^2)\epsilon_{x0}}} \int\int dI_z\, d\phi_z \Psi_z(t) \left[(1-\theta_x^2)\sin(\Phi_0 - \frac{\xi(z-z_0)}{R\alpha}) - 2\theta_x \cos(\Phi_0 - \frac{\xi(z-z_0)}{R\alpha})\right] \quad (33)$$

with

$$\Phi_0 = \omega_{x0}t + \phi_0 - \frac{\theta_x I_{x0}}{\epsilon_{x0}(1+\theta_x^2)} \quad \text{and:} \quad \theta_x = \mu_x \epsilon_{x0}\omega_x t$$

The contribution over $\int d\phi_z dI_z \Psi_z(t)\sin(\frac{\xi}{R\alpha}(z - z_0))$ vanishes as the distribution function is symmetric w.r.t. z. What remains is equal to:

$$< x >= \frac{\sqrt{2I_{x0}\beta}}{(1+\theta_x^2)^2} e^{-\frac{\theta_x^2 I_0}{(1+\theta_x^2)\epsilon_{x0}}} \Big[(1-\theta_x^2)\sin(\Phi_0) - 2\theta_x\cos(\Phi_0)\Big]\,\mathcal{E}(t) \qquad (34)$$

with the "envelope function" defined as:

$$\mathcal{E}(t) = \int\int dI\, d\phi\, \Psi(t) \cos(\frac{\xi}{R\alpha}(z - z_0)) \ . \tag{35}$$

At this point we have dropped the subscripts $\phi_z, I_z, \Psi_z \rightarrow \phi, I, \psi$. The term $\mathcal{E}(t)$ acts like a slow modulation on the decoherence of the betatron oscillations due to transverse nonlinear fields. We express $z - z_0$ in action-angle variables as shown in Eq. 32 and obtain with the distribution function from Eq. 11 for the envelope function:

$$\mathcal{E}(t) = \frac{1}{2\pi\sigma_{z0}\sigma_{\epsilon 0}} \int_0^\infty dI\, R(I) e^{-\frac{1+g^2}{2g\sigma_{z0}\sigma_{\epsilon 0}} I} \tag{36}$$

with

$$R(I) = \int_0^{2\pi} d\phi\, \cos(b \sin(\phi - \omega_s(I)t/2)) e^{-\frac{1-g^2}{2g\sigma_{z0}\sigma_{\epsilon 0}} I \cos(2\phi - 2\bar{\phi})} \quad \text{and} \quad b = \xi\sqrt{\frac{2I}{R\alpha\nu_s}} 2\sin(\omega_s(I)t/2) \ . \tag{37}$$

We shift the integration variable in Eq. 37 to: $\phi' = \phi - \omega_s(I)t/2 - \pi/2$ and have:

$$R(I) = \int_0^{2\pi} d\phi'\, \cos(b\cos(\phi')) e^{-\frac{1-g^2}{2g\sigma_{z0}\sigma_{\epsilon 0}} I \cos(2\phi' - 2\tilde{\phi})} \quad \text{with} \quad 2\tilde{\phi} = \omega_s(I)t + \pi \tag{38}$$

We compare this relation to the following equation which is proven in the appendix:

$$\int_0^{2\pi} d\phi \cos(\, b\cos(\phi)) e^{-a\cos(2\phi - 2\bar{\phi})} = 2\pi\Big[J_0(b)J_0(ia) + 2\sum_1^\infty (-i)^n J_n(ia) J_{2n}(b)\cos(2n\bar{\phi})\Big] \ , \tag{39}$$

and obtain finally for Eq. 38:

$$R(I) = 2\pi\Big[J_0(b)J_0(ia) + 2\sum_1^\infty (i)^n J_n(ia) J_{2n}(b)\cos(2n\hat{\phi})\Big] \ , \tag{40}$$

with

$$a = \frac{1-g^2}{2g\sigma_{z0}\sigma_{\epsilon 0}} I \quad \text{and} \quad 2\hat{\phi} = \omega_s t - \omega_s \mu I t \tag{41}$$

The integral over the action variable in Eq. 36 is done by means of the formula in Ref. [11]:

$$\int_0^\infty dI\, e^{-\bar{\alpha}I} J_n(\sqrt{I}\bar{a}i) J_{2n}(2\bar{b}I) \ = \ e^{-\frac{\bar{b}^2\bar{\alpha}}{\bar{\alpha}^2 - \bar{a}^2}} J_n(i\frac{\bar{b}^2\bar{a}}{\bar{\alpha}^2 - \bar{a}^2})(\bar{\alpha}^2 - \bar{a}^2)^{-1/2} \ .$$

and the envelope function becomes:

$$\mathcal{E}(t) = e^{-\kappa_t^2(1+g^2)}\Big[J_0(\kappa_t^2(1-g^2)) + 2\sum_{n=1}^\infty \cos(\omega_{s0}tn)\Re\Big\{X_n\Big\} - \sin(\omega_{s0}tn)\Im\Big\{X_n\Big\}\ \Big] \ , \tag{42}$$

with

$$X_n = (-i)^n e^{-\kappa_t^2(2ing\theta_z)} \frac{J_n(i\kappa_t^2(1-g^2)/Z_n)}{\sqrt{Z_n}} \ , \quad Z_n = 1 - \theta_z^2 n^2 + \frac{in\theta_z(1+g^2)}{g} \ , \quad \kappa_t = \frac{\sigma_{\epsilon 0}\sin(\omega_{s0}t/2)}{\nu_s} \tag{43}$$

where θ_z is the same expression that has been defined as θ in Eq. 12. We realize that κ_t is oscillating with time which causes the decoherence and recoherence phenomenon observed in the storage ring Alladin [16]. From Eq. 34 combined with Eq. 42 we notice the appearance of synchrotron sidebands to the betatron tune: $\omega_x \pm n\omega_s$. These sidebands should be visible in the Fourier spectrum of the injected center of mass motion. The quantity $\theta_z = \omega_{s0}\mu\sigma_{z0}\sigma_{\epsilon 0}t$ is proportional to the elapsed time after injection. Hence

$$\lim_{t\rightarrow\infty} |Z_n| = \lim_{t\rightarrow\infty} \sqrt{1 + \theta_z^4 n^4 + \theta_z^2 n^2 \frac{g^4+1}{g^2}} = \infty \ ,$$

and the contribution due to X_n in Eq.42 tends to zero after a sufficient number of revolutions. If we neglect the nonlinear fields of the synchrotron motion: $\theta_z = 0$ the envelope function becomes:

$$\mathcal{E}(t) = e^{-\kappa_t^2(1+g^2)} J_0(\kappa_t^2(1-g^2)) + 2\sum_{n=1}^{\infty} \cos(\omega_s t n) i^n J_n(i\kappa_t^2(1-g^2)) \ . \tag{44}$$

This series involving Bessel functions may be replaced by the generating function: $\exp(-\kappa_t^2(1-g^2)\cos(\omega_s t/2))$ (see [11]), and the envelope function simplifies to:

$$\mathcal{E}(t) = e^{-\kappa_t^2(1+g^2+(1-g^2)\cos(\omega_s t))} \tag{45}$$

This relation was already derived in [5] for a matched longitudinal phase space distribution $g = 1$.

Summary and Conclusion

We derived the evolution of the distribution function after mismatched and off-centered injection under the influence of nonlinear fields. The analytic expressions for the first and second moments of the distribution could be compared with beam position monitors, beam size (synchrotron light camera) and bunch length (streak camera) measurements. As a result these methods could be used to optimize injection into a circular accelerator.

However, we neglected radiation damping and these results are only valid for a time period which is significantly smaller than the radiation damping time. A more complete analysis which includes synchrotron radiation effects would involve the Fokker-Planck Equation [17].

Another type of application not mentioned in this paper addresses coherent instabilities. The unperturbed (i.e. zero current limit) distribution function derived here could be used to calculate the initial growth rate or the stability limit for a perturbed distribution function in the injection process.

Acknowledgement

I want to thank Sam Heifets, Martin Lee, Sankaranarayana Rajagopalan, Jim Spencer and Tor Raubenheimer for helpful discussions. My thanks are due to Ron Ruth whose encouragement was of great value during this work.

Appendix: Proof of Eq. 39

We want to proof the relation:

$$R(I) = \int_0^{2\pi} d\phi \cos(\, b\cos(\phi))e^{-a\cos(2\phi-2\bar{\phi})} = 2\pi\left[J_0(b)J_0(ia) + 2\sum_1^{\infty}(-i)^n J_n(ia)J_{2n}(b)\cos(2n\bar{\phi})\right] \tag{46}$$

First we expand the cosines in a power series:

$$R(I) = \sum_{n=0}^{\infty}(-1)^n\frac{b^{2n}}{(2n)!}\int_0^{2\pi} d\phi\cos(\phi))^{2n}\, e^{-a\cos(2\phi-2\bar{\phi})}\ . \tag{47}$$

Next we convert the powers of the cosines into a sum of trigonometric functions:

$$\cos(\phi)^{2n} = \frac{1}{2^{2n}}\sum_{k=0}^{2n}\left(\begin{array}{c}2n\\k\end{array}\right)\cos(2\phi(n-k))\ .$$

This relation may be found in [11]. We change the integration variable in Eq. 47 from ϕ to $\varphi = 2\phi - 2\bar{\phi}$ to simplify the exponent.

$$R(I) = \sum_{n=0}^{\infty}\frac{(-1)^n b^{2n}}{(2n)!2^{2n}}\sum_{k=0}^{2n}\left(\begin{array}{c}2n\\k\end{array}\right)\int_0^{2\pi} d\varphi\cos((n-k)(\varphi+2\bar{\phi}))e^{-a\cos(\varphi)} \tag{48}$$

We split the cosines function into:

$$\cos((n-k)(\varphi+2\bar{\phi})) = \cos((n-k)\varphi)\,\cos((n-k)2\bar{\phi}) - \sin((n-k)\varphi)\,\sin((n-k)2\bar{\phi})$$

The integration over the sines function vanishes due to symmetry. Now we integrate over ϕ using the Bessel function [11]:

$$\int_0^{2\pi} d\varphi\cos(m\varphi)e^{i\beta\cos(\varphi)} = 2\pi i^m J_m(\beta)$$

with $\beta = ia$ we obtain from Eq. 48:

$$R(I) = 2\pi\sum_{n=0}^{\infty}\frac{(-1)^n b^{2n}}{(2n)!2^{2n}}\sum_{k=0}^{2n}\left(\begin{array}{c}2n\\k\end{array}\right) i^{n-k}\cos(2\bar{\phi}(n-k))\,J_{n-k}(ia)\ . \tag{49}$$

Let us write this relation in a more compact form:

$$R(I) = \sum_{n=0}^{\infty}B_n\sum_{k=0}^{2n}\frac{C_{n-k}}{(2n-k)!\,k!}\ , \tag{50}$$

where we used:

$$C_{n-k} = i^{n-k}\cos(2\bar{\phi}(n-k))\,J_{n-k}(ia) \qquad \text{and} \qquad B_n = \frac{(-1)^n b^{2n}}{2^{2n}} \tag{51}$$

We substitute $m = n - k$ From Eq. 50 we obtain due to the symmetry $C_{n-k} = C_{k-n}$:

$$R(I) = \sum_{n=0}^{\infty}B_n\left[\frac{C_0}{n!\,n!} + 2\sum_{m=1}^{m\le n}\frac{C_m}{(n+m)!\,(n-m)!}\right] \tag{52}$$

In Eq. 52 we sum over a triangular shaped field in the dimensions n and m:

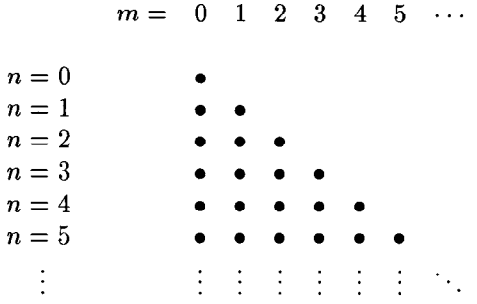

The summation in Eq. 52 is done first horizontally in the sketched triangle, over m, and then vertically, over n. We switch now the sequence of summation between n and m and rewrite Eq. 52 as:

$$R(I) = \sum_{n=0}^{\infty} B_n \frac{C_0}{n!\,n!} + 2\sum_{m=1}^{\infty}\sum_{n\geq m}^{\infty} \frac{B_n C_m}{(n+m)!\,(n-m)!} \tag{53}$$

With B_n from Eq. 51 the summation over n becomes:

$$\sum_{n\geq m}^{\infty} \frac{B_n}{(n+m)!\,(n-m)!} = (-1)^m \sum_{n'=0}^{\infty} (-1)^{n'} \frac{b^{2n'+2m}}{(n'+2m)!\,(n')!\,2^{2n'+2m}} = (-1)^m J_{2m}(b)\ , \tag{54}$$

where we used the power series representation of the Bessel function [11]:

$$J_m(z) = \frac{z^m}{2^m}\sum_{k=0}^{\infty}(-1)^k \frac{z^{2k}}{2^{2k}k!(m+k)!}\ .$$

With Eq. 53 and C_m form Eq. 51 we obtain

$$R(I) = 2\pi\left[J_0(b)J_0(ia) + 2\sum_{m=1}^{\infty}(-i)^m J_m(ia)J_{2m}(b)\cos(2m\bar{\phi})\right]$$

which is the relation we wanted to proof.

References

[1] Matt Sands, *The Physics of Electrons Storage Rings* SLAC-121, Nov (1970).

[2] Tor Raubenheimer, *The Generation and Acceleration of Low Emittance Flat Beams for Future Linear Colliders,* SLAC-387, Nov (1991).

[3] Nikolitsa Merminga, *A Study of Nonlinear Dynamics in the Fermilab TEVATRON,* FNAL-508, Jan (1989).

[4] Nicholas Savill, *Smear Studies for the Dynanic Aperture Experiment,* CERN SL-AP Note 90-19, July (1991).

[5] R. E. Meller, A. W. Chao, J. M. Peterson, S. G. Peggs and M. Furman, *Decoherence of Kicked Beams,* SSC N 360, May (1987).

[6] V. I. Arnold, *Dynamical Systems III,* Springer Verlag, Berlin, (1985).

[7] T. Suzuki, *Hamilton Formulation for Synchrotron Oscillations and Sacherer's Integral Equation,* Particle Accelerators, **12**, pp. 237 (1982).

[8] Ron Ruth, *Nonlinear Dynamics Aspects of Particle Accelerators,* Springer Lecture Notes 247, Proceedings, Sardinia (1985).

[9] E. D. Courant, *et al* , *Stability in Dynamical Systems,* SLAC-PUB 3415, Aug (1984).

[10] G. Gallavotti, *The Elements of Mechanics,* Springer Verlag New York, (1983).

[11] I. Gradstein and I. Ryshik, *Tables of Series, Sums and Integrals,* Harri Deutsch, Thun Frankfurt, (1981).

[12] F. C. Iselin *The MAD Program,* CERN/SL/90-13, (1990).

[13] J. P. Delahaye and L. Rivkin, *SLC Positron Damping Ring Optics Design,* IEEE Trans. Nucl. Sci. **32**, pp. 1695 (1985).

[14] N. Merminga *et al* , *Transverse Phase Space in the Presence of Dispersion,* SLAC-PUB 5514, May (1991).

[15] F. J. Decker *et al* , *Dispersion and betatron Matching into the Linac* SLAC-PUB 5484, May (1991).

[16] Ian C. Hsu, *The Decoherence and Recoherence of the Betatron Oscillation Signal and an Application,* Particle Accelerators, **34**, pp. 43 (1990).

[17] H. Moshammer, *Application of the Fokker-Planck Equation to Particle Beams injected into Damping Rings,* in preparation, May (1992).